Journal of Advanced Research in Fluid Mechanics and Thermal Sciences

Journal homepage:
https://semarakilmu.com.my/journals/index.php/fluid_mechanics_thermal_sciences/index
ISSN: 2289-7879

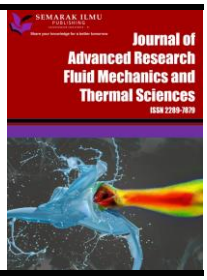


# Influence of Leading and Trailing Edge Angle on Impeller Blades of a Pump as Turbine

Diego Penagos-Vasquez[1,*], Jonathan Graciano-Uribe[2], Luis Grisales-Noreña[3], Sebastián Vélez García[1], Edward Andrés Torres-López[4]

[1] Faculty of Engineering, Department of Mechatronics and Electromechanics, Research group – MATyER, Instituto Tecnológico Metropolitano, 050034 Medellín, Colombia
[2] Department of Mechanical Engineering and Industrial Construction, University of Girona, c/ Universitat de Girona 4, 17003 Girona, Catalonia, Spain
[3] Department of Electrical Engineering, Faculty of Engineering, Universidad de Talca, Curicó 3340000, Chile
[4] Department of Mechanical Engineering, University of Antioquia - Research group GEA, Medellín, Antioquia, Colombia

**ARTICLE INFO**

***Article history:***
Received 25 November 2022
Received in revised form 22 March 2023
Accepted 30 March 2023
Available online 19 April 2023

***Keywords:***
Impeller; hydraulic efficiency; pump as turbine; leading edge; trailing edge

**ABSTRACT**

A pump as turbine (PAT) is a turbomachine that converts hydraulic energy into electricity. One of the study topics in PAT is the efficiency due to centrifugal pumps are not designed to operate in reverse mode. Geometric variations of the impeller have been studied in the literature. However, it was not possible to evidence the influence of the inclination of the blade leading and trailing edge. Therefore, the objective of this work is to analyze numerically and fluid dynamically the inclination angle of the blade leading and trailing edge of a centrifugal pump, in pump and turbine mode. First, the characteristic curve was validated. Then, the inclination of the leading and the trailing edge was modified, in a range of 25° to 90°, obtaining head, efficiency, and power graph. As a result, in pump mode was evidenced that an angle close to 90° on the blade trailing edge provides a higher efficiency of 50.26% and decreases until 40.77% when the angle approaches 30°, reducing the head to around 20%, while power remained constant. In turbine mode, an inverse effect was obtained, where the maximum efficiency was 60.9% and the generated power increased up to 4.76 kW in the blade leading edge. Therefore, the angular variation of the leading and the trailing edge is adequate in turbine mode, while in pump mode there is a loss of capacity.

## 1. Introduction

### *1.1 General Context*

A centrifugal pump is a turbomachine that converts the kinetic energy of a fluid into pressure [1]. PAT (Pump as Turbine) refers to the reverse operation of a conventional centrifugal pump, i.e., the turbomachine receives the pressure energy coming from the water and transforms it into rotational mechanical energy, which can be harnessed by connecting a generator in small hydroelectric power plants [2]. PATs are adaptable to other renewable energy systems, such as wind and photovoltaic

* *Corresponding author.*
*E-mail address: diegopenagos@itm.edu.co*

https://doi.org/10.37934/arfmts.105.1.166183

farms. In addition, pumped-storage hydroelectricity, which uses PATs, stabilizes electricity with variations from other sources [3,4].

### *1.2 Issue and Motivation*

The issue presented by PATs is that the turbomachinery is not designed to operate in reverse, which is why manufacturers do not report the operating curve in turbine mode [5]. Furthermore, the site conditions at the best efficiency point (BEP) in turbine mode are superior to the conditions of operation in pump mode. An experimental study conducted by Barbarelli *et al.,* [6] obtained as a result a minimum 15% increase in hydraulic head and flow rate for 12 turbomachines analyzed. In the same way, Derakhshan and Nourbakhsh [7] showed a 33% increase in head and an 11% in flow rate for 11 PATs analyzed. Therefore, the operating conditions in turbine mode were superior to pump mode. On the other hand, the efficiency in turbine mode is lower than in pump mode. This has been evidenced in numerical and experimental studies, where the turbine mode efficiency was found to be 4.9% lower, 1.1%, and 10.8% [8-10]. In contrast, Miao *et al.,* [11], achieved a 4.6% increase in turbine mode operation. However, they did not consider the technical operating conditions of the turbomachinery. Therefore, based on the research conducted so far, a versatile impeller for operation in both flow directions has not been developed. Based on the above, studies focus on improving efficiency in turbine mode without affecting efficiency in pump mode. For this purpose, investigations have carried out computational fluid dynamics simulations (CFD) to obtain the turbine mode operating curve. On the other hand, to evaluate the behavior of the PAT, geometric variations in the impeller have been investigated to obtain a versatile impeller for both modes of operation and determine its performance.

### *1.3 State of the Art*

Based on the computational simulation, a literature review carried out by Plua *et al.,* [12] showed that 80% of the numerical studies were performed in ANSYS software, while the preceding programs are FloEFD and OpenFoam with 6%. ANSYS has been widely used software for similar analyses, such as in spiral chambers, H-Darrieus turbines, and propeller-type turbines [13-15]. Moreover, 58% of the researchers used the $k-\varepsilon$ turbulence model, followed by the $k-\omega-SST$ model with 27% of the application. On the other hand, Barbarelli *et al.,* [5] evaluated 12 radial pumps in both operation modes, obtaining the experimental characteristic curve for further studies. Fernández *et al.,* [16] validated the characteristic curve with experimental data, using five different BEP flow rates. They obtained a maximum relative error of 9%. Yang *et al.,* [8] performed the validation of the characteristic curve comparing empirical relationships, obtaining an error of less than 3.33%. Other validations found have obtained errors of 12%, 5-10%, 7.41%, and 4%, concerning efficiency [17-20].

Regarding the geometrical modification of the impeller, the variation of different parameters in the efficiency evaluation has been investigated. Derakhshan *et al.,* [21] modified the leading edge, applying a rounding. As a result, the PAT efficiency increased up to 5.5%. Yang *et al.,* [22] used different wrap angles. The researchers found that for a specific speed of 46.15, the efficiency reached 82.04% at 60°. Li *et al.,* [23] varied the blade outlet width obtaining an efficiency of 57.2% for a 13 mm thick blade. Peng *et al.,* [24] used different blade outlet angles, ranging from 16°-32°. The authors found that a better anti-cavitation effect is achieved at 16°. Finally, Sen-Chun *et al.,* [25] modified the curvature of the hydraulic profile by employing a genetic algorithm, obtaining a 3.62% increase in efficiency.

From the studies presented in the state of the art, it was not possible to evidence the influence on the angle of inclination of the blade leading and trailing edge and its hydraulic behavior. Therefore, how can this variation affect the efficiency, power, and head of a PAT? The objective of this research was the numerical analysis of the inclination angle of the leading and trailing edge of the impeller blades of a radial flow PAT, in pump and turbine mode. Consequently, computational tools were applied to a commercial pump impeller, using concepts of fluid mechanics and fluid-dynamic analysis. Finally, this study allowed exploring new parameters that will serve to broaden the scientific field in the study of PATs.

### *1.4 Main Contributions*

Considering the review of the state of the art presented above, the main contributions of this paper are listed below

i. Clearly supply to the scientific literature with the effects that the modification of the angles of the leading and trailing edge has on the performance of a PAT for both operation modes, since in the scientific literature most of the efforts have been focused on the implementation of rounding in these zones.
ii. Provide a numerical strategy that allows future research in the field of PAT to predict its behavior in turbine mode, starting from the characteristic curve in pump mode, since the manufacturers supply such information at the time of acquisition, but do not have the characterization of the turbomachine in turbine mode.
iii. Offer a high level of numerical reliability to the previously mentioned contributions by considering within the analysis the GCI methodology based on Richardson's extrapolation method, a method that currently offers better results than the classical mesh independence study strategies used in most of the studies reported in the field of PAT.

## 2. Methodology

Figure 1 shows the proposed procedure for the evaluation of the inclination angle of the blade leading and trailing edge, in pump and turbine mode. It starts by extracting the BEP data from the characteristic curve provided by the pump manufacturer. Subsequently, the impeller and volute are modeled. Then, both geometries are discretized. Next, the boundary conditions are established, based on the manufacturer's curve. Then, the simulation is validated with the characteristic curve. If an error of less than 10% is obtained at BEP, the geometry variation of the blade leading and trailing edge is modified. Finally, the boundary conditions are established in turbine mode, and validated and the above-mentioned geometrical variation is performed.

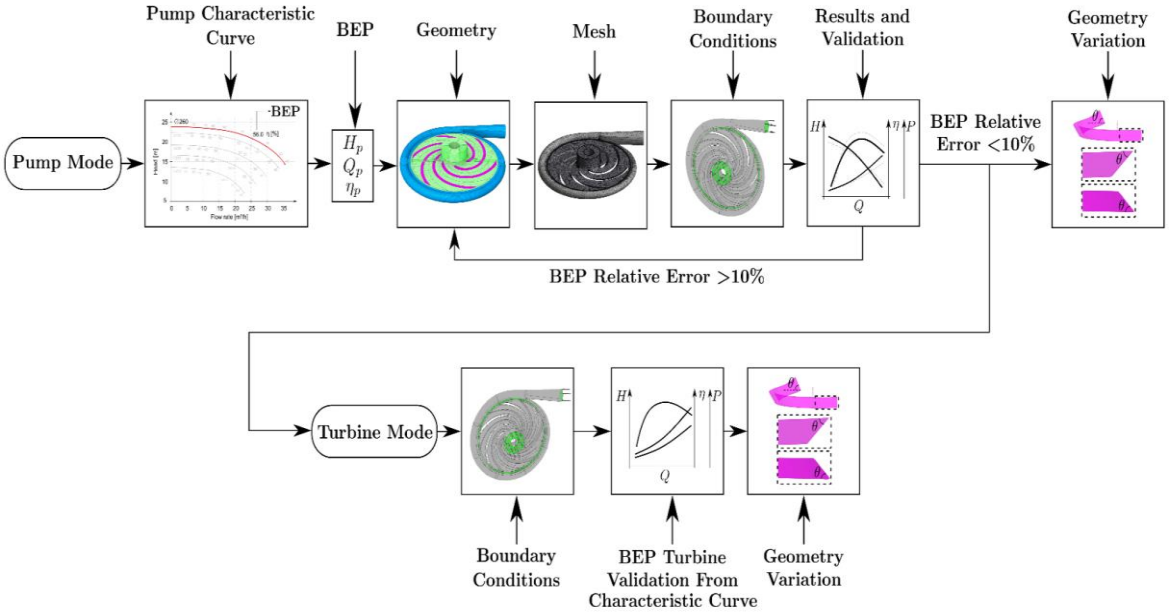


**Fig. 1.** General methodology of the proposed investigation

## *2.1 Study Case*

Figure 2 shows the characteristic curve of the commercial pump used, which relates flow rate to the head and hydraulic efficiency. The curve highlighted in red, which has a 260 mm diameter impeller, was used in this investigation. In addition, 7 points were used in the numerical simulation. The schematic pump image is shown on the right. Table 1 shows the BEP data and geometrical parameters of the turbomachine, along with the manufacturer's information [26]. The turbomachine evaluated in this study was analyzed in a previous publication for obtaining the turbine-mode characteristic curve [27].

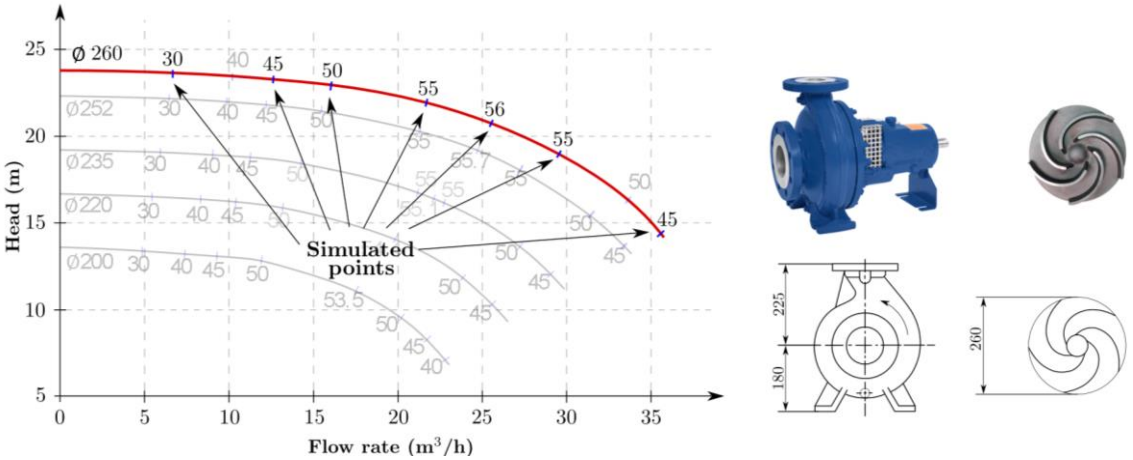


**Fig. 2.** Pump characteristic curve and schematic diagram

**Table 1**
Pump specifications

| Concept | Detail |
|---|---|
| Manufacturer | KSB |
| Reference | MegaCPK 065-040-250 |
| Flow Type | Radial |
| Flow rate at BEP ($m^3/h$) | 25.49 |
| Head at BEP (m) | 20.71 |
| Efficiency at BEP (%) | 56.0 |
| Rotational Speed (rpm) | 1450 |
| Suction Diameter (mm) | 65 |
| Discharge Diameter (mm) | 40 |
| Impeller Inlet Radius $r_1$ (mm) | 32.5 |
| Impeller Outlet Radius $r_2$ (mm) | 130 |
| Impeller Shaft Radius $r_{sh}$ (mm) | 16 |
| Blade Outlet Width $b_2$ (mm) | 8 |
| Blades | 6 |

## *2.2 Computational Modeling*

Figure 3 shows the representation of the hydraulic profile of the impeller from a three-dimensional view. A closed impeller is shown on the left, where the shroud covers the blades. Next, in the middle, the computational model of the impeller is presented, without the top cover, where the blades are visualized. An outline of lines of different colors can be seen highlighting one of the blades. Finally, on the right, it is possible to observe the hydraulic profile or meridional view, positioned in a two-dimensional plane. This research focused on the angular variation of the leading edge (LE) and trailing edge (TE). Both points are named depending on the operation of the turbomachine. The representation of the hydraulic profile is necessary since it is a geometric simplification of a three-dimensional plane.

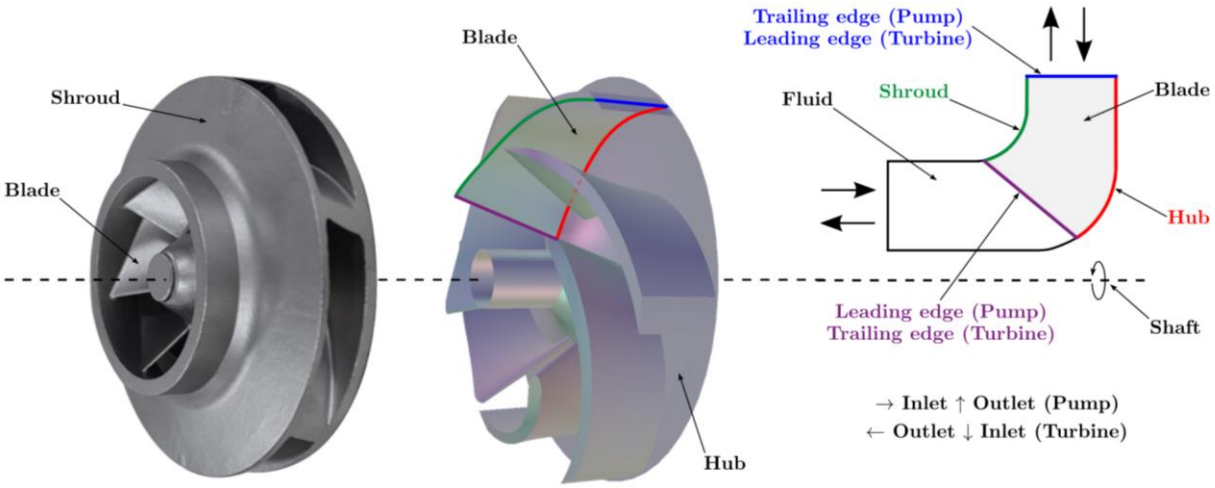


**Fig. 3.** Hydraulic profile from the three-dimensional view of the impeller

The computational modeling was performed in Ansys 2023 R1 software. The BladeDesign module was used to generate the hydraulic profile, where the BEP data, water density, rotation speed, and the number of blades were provided. The software calculated an approximate control volume of the impeller section, volute, and blades. The hydraulic profile is then adjusted to ensure that the computational model is close to the real one. Figure 4 shows the result of the computer modeling,

where the assembly of the volute, impeller, and blades (left) is shown close to a cross-section, exposing the hydraulic profile view (right).

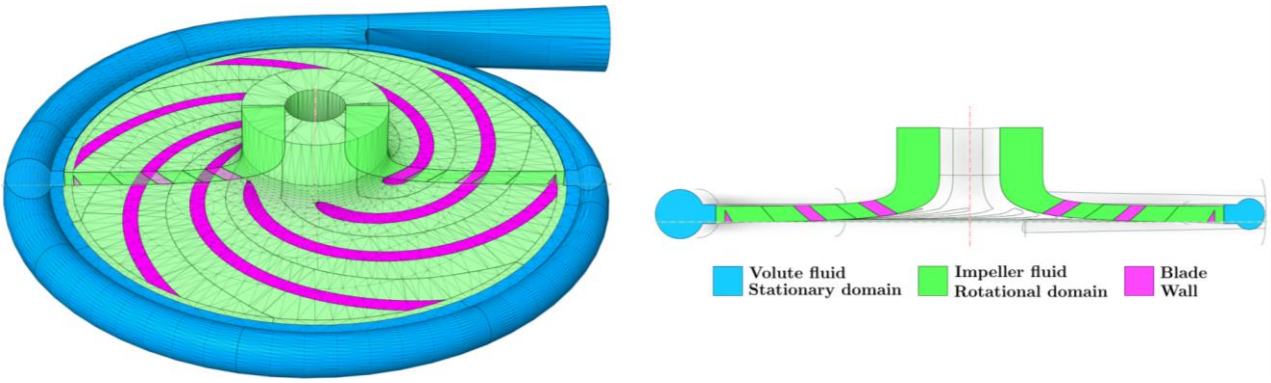


**Fig. 4.** Computational model of the centrifugal pump

### *2.3 Mesh*

In the discretization of the geometry in Figure 4, a mesh study was conducted using the grid convergence index (GCI). GCI is based on the Richardson extrapolation method [28]. This method allows estimating an exact solution of a fluid-dynamic variable when the number of mesh elements tends to infinity. Additionally, it determines an appropriate mesh for further simulations. In the literature, studies have been conducted on gravitational vortex turbines, and PATs, analyzing variables such as head, torque, and time step [29-31].

Table 2 presents the results obtained for the three analyzed meshes in terms of head, efficiency, and power, based on the formulation presented in the Richardson extrapolation method. Figure 5 shows the graphs depicting the convergence behavior of the extrapolated variable concerning the representative grid size. After analyzing the Richardson extrapolation, it was determined that a mesh of 1,024,849 elements was a suitable option due to GCI lower than 0.5%. The chosen mesh has slight deviations from the Richardson extrapolation solution, but it still effectively reduced the computational time.

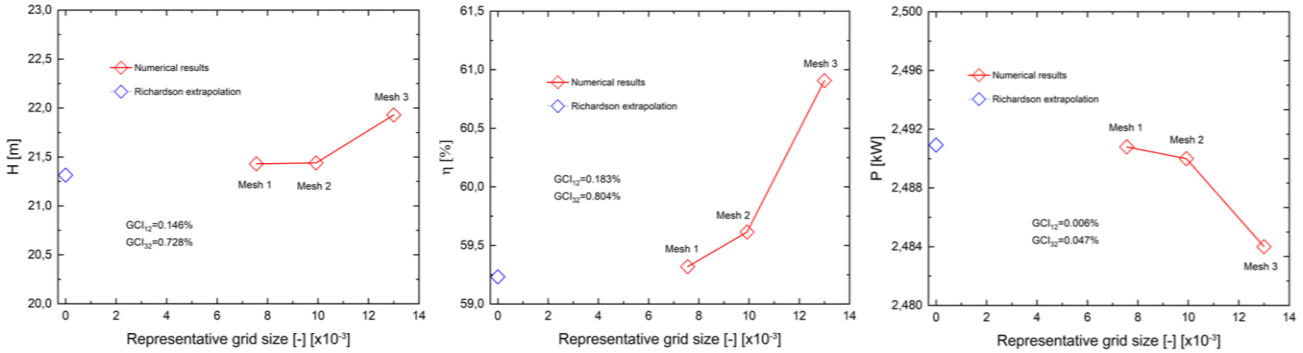


**Fig. 5.** Mesh independence of head, efficiency, and power

**Table 2**
Results for the mesh independence using the Richardson extrapolation method

| Concept | Head | Efficiency | Power | Detail |
|---|---|---|---|---|
| $N_1$ | 2,314,498 | 2,314,498 | 2,314,498 | Fine mesh |
| $N_2$ | 1,024,849 | 1,024,849 | 1,024,849 | Medium mesh |
| $N_3$ | 454,976 | 454,976 | 454,976 | Coarse mesh |
| $h_1$ | 0.00756 | 0.00756 | 0.00756 | Fine representative grid size |
| $h_2$ | 0.00992 | 0.00992 | 0.00992 | Medium representative grid size |
| $h_3$ | 0.0130 | 0.0130 | 0.0130 | Coarse representative grid size |
| $r_{21}$ | 1.311 | 1.311 | 1.311 | Refinement factor ($\geq 1.3$) |
| $r_{32}$ | 1.311 | 1.311 | 1.311 | Refinement factor ($\geq 1.3$) |
| $\phi_1$ | 21.430 | 59.319 | 2490.8 | Analyzed variable |
| $\phi_2$ | 21.439 | 59.614 | 2490.0 | Analyzed variable |
| $\phi_3$ | 21.930 | 60.907 | 2484.0 | Analyzed variable |
| $p$ | 5.896 | 5.451 | 7.420 | Apparent order |
| $e_a^{21}$ (%) | 0.464 | 0.496 | 0.032 | Relative error of analyzed variable |
| $e_a^{32}$ (%) | 2.290 | 2.169 | 0.241 | Relative error of analyzed variable |
| $\phi_{ext}^{21}$ | 21.315 | 59.232 | 2490.923 | Extrapolated value for $h = 0$ |
| $\phi_{ext}^{32}$ | 21.314 | 59.230 | 2490.929 | Extrapolated value for $h = 0$ |
| $e_{ext}^{21}$ (%) | 0.117 | 0.146 | 0.005 | Relative error considering extrapolated value |
| $e_{ext}^{32}$ (%) | 0.586 | 0.647 | 0.037 | Relative error considering extrapolated value |
| $GCI_{12}$ (%) | 0.146 | 0.183 | 0.006 | Fine-grid convergence index |
| $GCI_{32}$ (%) | 0.728 | 0.804 | 0.047 | Coarse-grid convergence index |
| $GCI$ | 1.004 | 1.003 | 1.011 | The value must be $\approx 1.0$ |

The mesh was developed in the Meshing module of Ansys 2023 R1. Figure 6 shows the mesh selected in the Richardson extrapolation method. It is possible to see the impeller and volute, showing a close-up of details in cross-sections of the mesh assembly. Table 3 illustrates the mesh statistics and metrics, which relate to the minimum quality required by the Ansys-CFX solver [32].

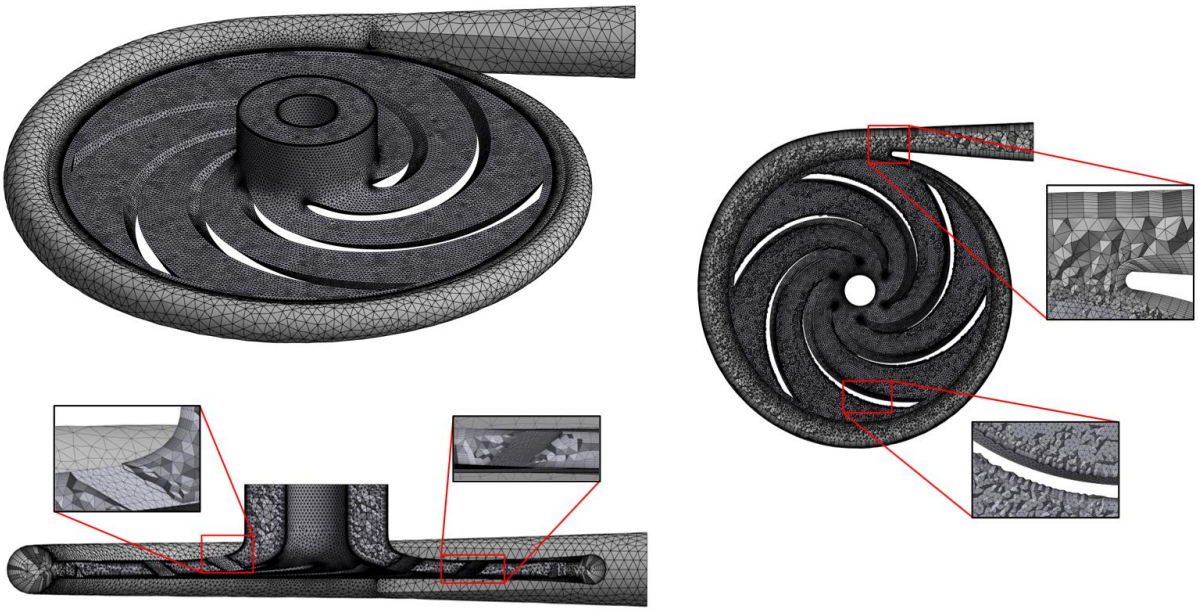

**Fig. 6.** Meshing of the impeller and volute control volume

**Table 3**
Mesh statistics and metrics

| Elements | | | Metrics | |
|---|---|---|---|---|
| Volume | Nodes | Elements | Concept | Value |
| Impeller | 124,104 | 601,182 | Aspect Ratio | 10.725 |
| Volute | 84,953 | 423,667 | Expansion | 17 |
| Total | 209,157 | 1,024,849 | Orthogonal Quality | 0.193 |

### *2.4 Governing Equations and Boundary Conditions*

The turbulence model used in this study was $k-\varepsilon$. This model solves two separate transport equations by considering the turbulent kinetic energy $k$ and dissipation $\varepsilon$ as unknowns. In addition, it considers the time-averaged fluid velocity [33]. Eq. (1) to Eq. (3) expresses the formulation of the stationary $k-\varepsilon$ model with its respective constants.

$$\frac{\partial(\rho k u_i)}{\partial x_i} = \frac{\partial}{\partial x_j}\left[\left(\mu + \frac{\mu_t}{\rho_k}\right)\frac{\partial k}{\partial x_j}\right] + P_k - \rho\varepsilon \tag{1}$$

$$\frac{\partial(\rho\varepsilon u_i)}{\partial x_i} = \frac{\partial}{\partial x_j}\left[\left(\mu + \frac{\mu_t}{\rho_\varepsilon}\right)\frac{\partial \varepsilon}{\partial x_j}\right] + C_{1\varepsilon}\frac{\varepsilon}{k}P_k - C_{2\varepsilon}\rho\frac{\varepsilon^2}{k} \tag{2}$$

$$\mu_t = \rho C_\mu \frac{k^2}{\varepsilon} = \frac{1}{2}\left(\frac{\partial u_j}{\partial x_i} + \frac{\partial u_i}{\partial x_j}\right) \tag{3}$$

Eq. (4) to Eq. (6) defines the turbulent kinetic energy and turbulent energy dissipation tensors, where the divergence operator is represented by the symbol $\nabla$ and u is the fluid velocity vector. A finite element analysis (FEA) can be applied to solve the system of equations. The $k-\varepsilon$ turbulence model is used to predict the flow behavior in bulk regions [34].

$$\begin{aligned}&\rho(\boldsymbol{u}\cdot\nabla)\boldsymbol{u} = \nabla\cdot[-p\boldsymbol{I} + (\mu+\mu_T)(\nabla\boldsymbol{u} + \nabla\boldsymbol{u}^T)]\\ &\nabla\cdot\boldsymbol{u} = 0\end{aligned} \tag{4}$$

$$\rho(\boldsymbol{u}\cdot\nabla)k = \nabla\cdot\left[\left(\mu + \frac{\mu_t}{\rho_k}\right)\nabla k\right] + P_k - \rho\varepsilon \tag{5}$$

$$\rho(\boldsymbol{u}\cdot\nabla)\varepsilon = \nabla\cdot\left[\left(\mu + \frac{\mu_t}{\rho_\varepsilon}\right)\nabla\varepsilon\right] + C_{1\varepsilon}\frac{\varepsilon}{k}P_k - C_{2\varepsilon}\rho\frac{\varepsilon^2}{k} \tag{6}$$

The $k-\varepsilon$ turbulence model has been used in this simulation because of its cost ratio, numerical results, and simulation efficiency, although it requires more mesh points and does not adequately capture the phenomena in the near-wall regions [35]. However, it is useful for free shear layer flows with small pressure gradients, while for larger gradients the accuracy of the results is reduced [36]. Several authors have used the $k-\varepsilon$ model because of the approximation with experimental results. Using the efficiency parameter, errors of 12% have been evidenced, 10%, and 4%, so using this model in centrifugal pumps is acceptable [17,37,38].

Two domains were configured: static for the volute and rotational for the impeller. The type of analysis was stationary. The relative pressure, set at 0 kPa, was selected as the input variable. The output variable was the mass flow rate, over the points of the characteristic curve. The density of water was 997.1 kg/m³, at 25°C, considering an isothermal process [39]. The impeller rotation speed

was 1450 rpm. The interface was Frozen Rotor, used for rotating turbomachines [40]. The residual value was $1\times10^{-6}$ and 1,000 iterations.

To construct the characteristic curve, Eq. (7) and Eq. (8) were set in the software. Using Eq. (7), the head $H$ *(m)* in both operation modes was determined by relating the outlet pressure $P_{outlet}$ *(Pa)* and inlet pressure $P_{inlet}$ *(Pa)* of the flow concerning the density $\rho$ *(kg/m³)* and gravity *g (m/s²)* [41,42]. Eq. (8) was used to calculate the efficiency in turbine mode $\eta_t$ *(%)* by relating the shaft power $P$ *(kW)* to density, gravity, head, and flow $Q$ *(m³/s)* [43,44].

$$\mathrm{H} = \frac{P_{outlet} - P_{inlet}}{\rho g} \tag{7}$$

$$\eta_t = \frac{P}{\rho g H Q} \tag{8}$$

### *2.5 LE and TE Variation*

After validating the behavior in pump mode, the inclination of the LE and TE was modified. Figure 7 presents the blade geometry scheme, together with the angle that was modified in pump or turbine mode, according to the flow direction. The view of the hydraulic profile is detailed, where it is shown in variable angle $\theta$. The first variation (left) was denoted as shroud LE and shroud TE in turbine mode. Also, it is possible to visualize one blade, together with a zoom that exposes the modified geometrical condition. The range varied for this case was 25°, 35°, 45°, 56.6°, 70°, and 90°, while the other angles were kept fixed at 90°. The other modifications were the variation of shroud TE in pump mode (shroud LE in turbine), and hub TE in pump mode (hub LE in turbine), where both were developed for values of 30°, 45°, 60°, 75°, and 90°, keeping the opposite angle of 25° fixed.

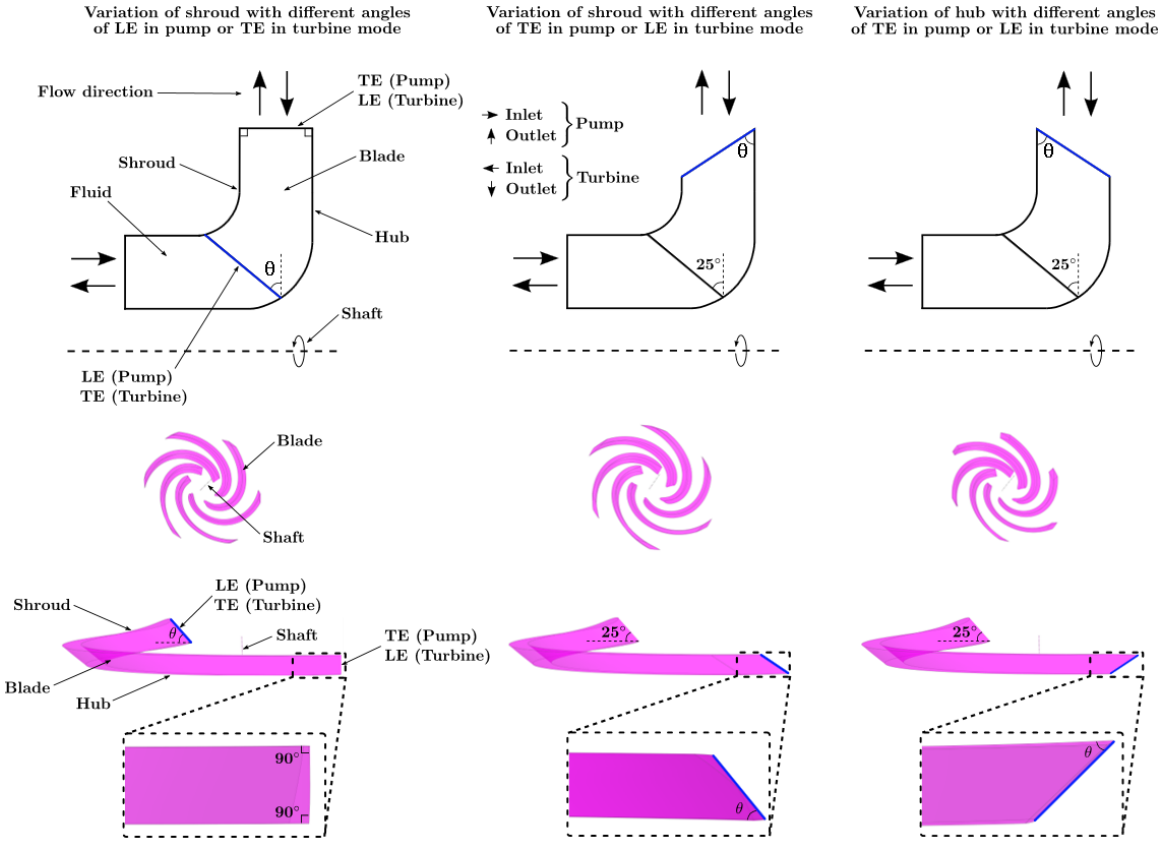


**Fig. 7.** Geometrical variation of LE and TE in both PAT operating modes

### *2.6 Turbine Mode*

The boundary conditions in turbine mode change concerning the inlet and outlet, where these two conditions are reversed. In a previous study by Vásquez *et al.,* [27], the BEP was calculated as H = 56.79 m, $Q$ = 49.99 m³/h, and $\omega$ = 1382 rpm. Based on the above, the inlet boundary (volute outlet) was used as mass flow, the outlet boundary (impeller inlet) as pressure, and the rotation at 1382 rpm. Upon validation of the above conditions, LE and TE were modified, as discussed in section 2.5.

## 3. Results and Discussion

### *3.1 Pump Mode*

The numerical results in pump mode are compared with the manufacturer's experimental curve, while in turbine mode were compared with the theoretical calculations of the previous study [27]. Figure 8 shows the comparison between the manufacturer's characteristic and the numerical curve. The head and efficiency curves are above the manufacturer's curve, while the power is below. At the BEP, CFD results were as follows: efficiency 59.52%, head 21.44 m, and power 2.49 kW. The trend of the head curve is decreasing, the efficiency curve is concave downward, and the power curve is increasing. It could be noticed that at 35 m³/h, the maximum relative error is 16.00% and the absolute error is 7.20%. On the other hand, the minimum relative error is 5.45% and the absolute error is 3.00%, at the previous point. In the BEP, the relative error in efficiency was 6.29% and the absolute error was 3.52%. As the points outside the BEP were analyzed, both parameters tend to increase. Finally, error bars were plotted on the manufacturer's efficiency curve, equivalent to a relative error obtained of 6.29%. This error is due to various factors, such as stationary simulation approach, mesh refinement, turbulence model, absence of thermal effects, and blade modeling.

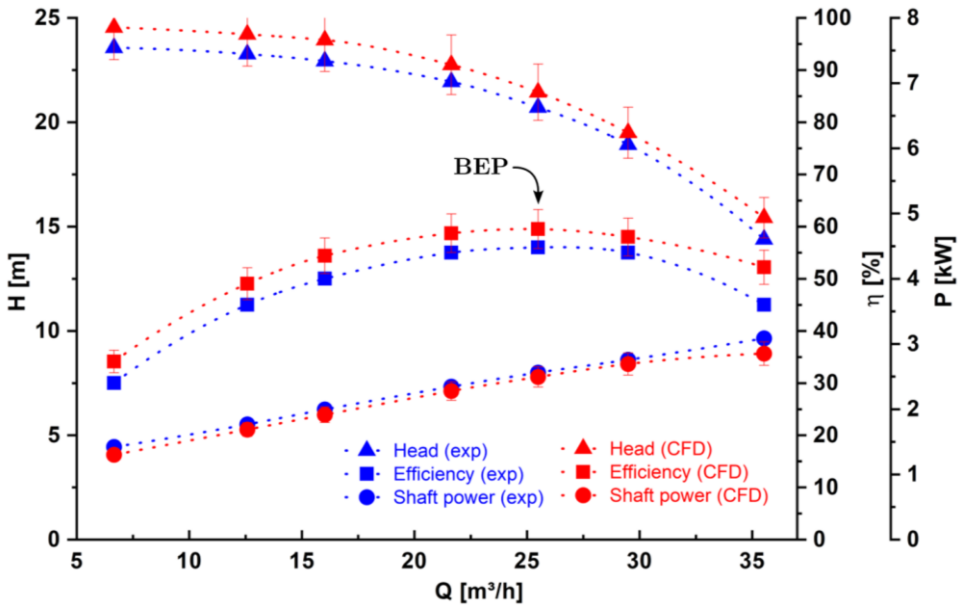


**Fig. 8.** Experimental and numerical characteristic curve [27]

Figure 9 shows the pressure and velocity contours of the fluid dynamic validation in the BEP, in the cross-section view, meridional view, blade-to-blade view, leading edge, and trailing edge. On the left, pressure contours of the PAT are observed. Pressure is in the range of 75.8 kPa to 313 kPa. In the suction, the pressure decreases to a value close to 75.8 kPa just as the fluid enters the impeller, and gradually increases in the volute to 313 kPa. However, the meridional view and blade-to-blade

view (allow for identifying the pressure behavior along the impeller) present maximum values close to 250 kPa, because the volute is the element in charge of receiving the kinetic energy of the impeller to transform it into pressure energy. The maximum pressure reached near the LE region was close to 100 kPa. This was due to the atmospheric pressure inlet condition. The pressure located at TE was around 250 kPa due to the interface between both components of the machine.

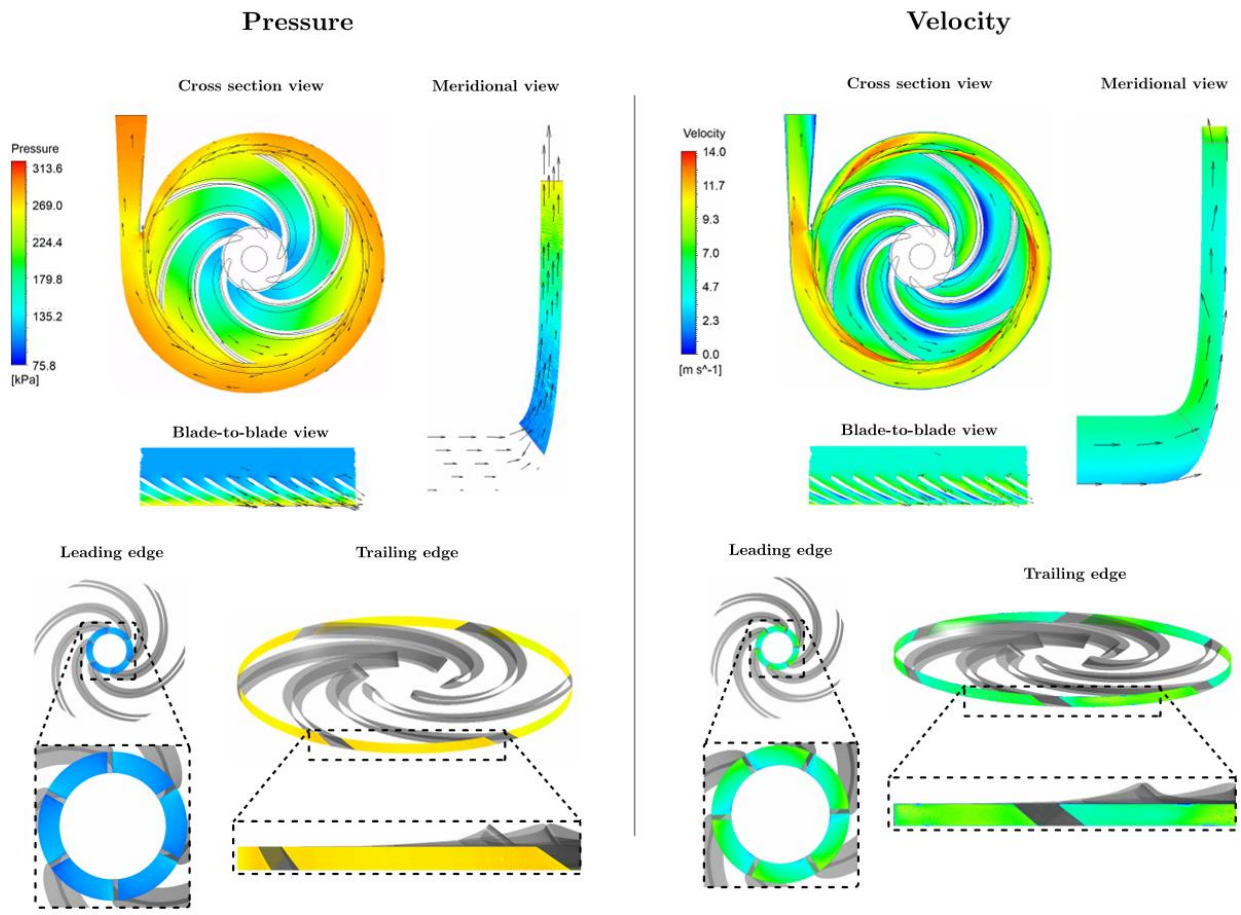


**Fig. 9.** Pressure and velocity contours in pump mode

On the right, velocity contours of the PAT are observed. Velocity is in the range of 0 m/s to 14 m/s. As the fluid enters the impeller, the velocity increases sharply to 14 m/s, due to rotation. Next, velocity suddenly decreases due to the energy transformation into pressure energy. The meridional view and blade-to-blade view present intermediate values close to 7 m/s. The LE and TE region obtained a velocity between 5 and 7 m/s. When the fluid enters the volute, the velocity decreases, being inverse to the pressure.

Figure 10 shows the behavior of inclination angle variation in LE and TE concerning head, efficiency, and power variables in pump mode. Due to the shroud LE having a special variation, the comparison point of 25° coincides with the simulation conditions of 90° for TE. An increasing trend in head and efficiency could be observed, which increases from 30° up to 90° by 16.4% and 17.6% more head pumping capacity in shroud TE and Hub TE. However, radial impellers are manufactured at 90°. On the other hand, the shroud LE curve has a behavior with negligible variations until 2.8%. With this, it can be stated that the impact on the behavior of the turbomachine in pump mode is not slightly affected by varying the LE while modifying the TE producing a decrease in the pumping capacity of the centrifugal pump. This behavior is similar in efficiency, where the curves have the

same trend. In this case, shroud TE and Hub TE had a difference of 17.6% and 18.9%, and 2.7% in shroud LE.

On the other hand, although there were minimal variations in the power curve, these are negligible when compared to the shaft scale. The maximum power difference was 1.6% in hub TE. Therefore, the power was not affected by the geometrical modification of LE and TE.

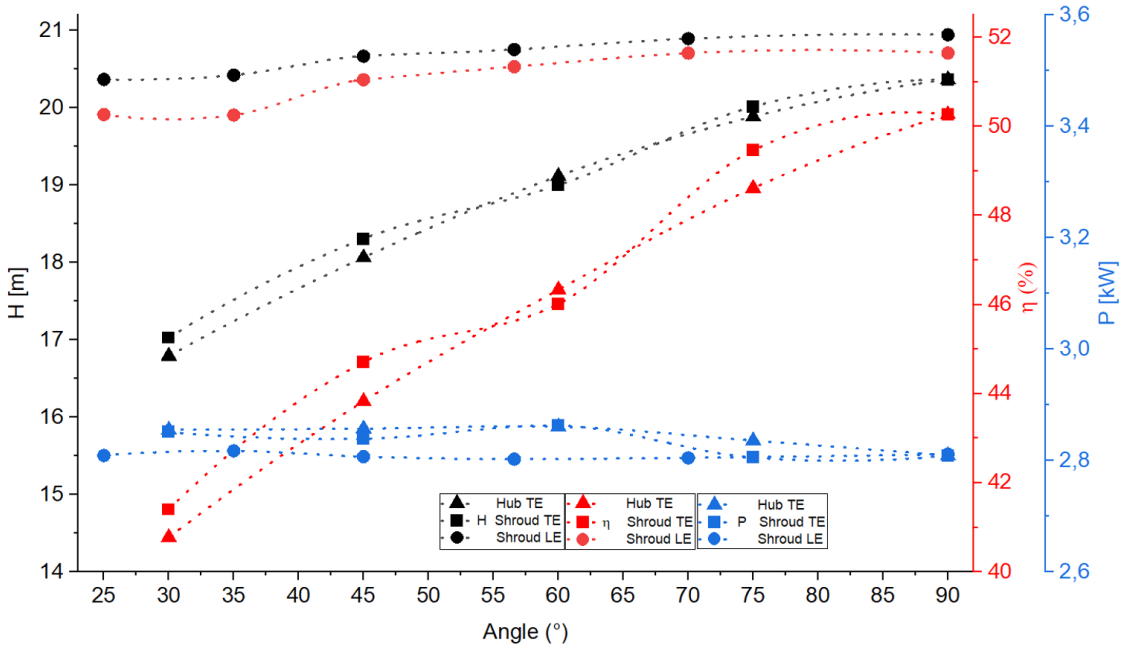


**Fig. 10.** Inclination angle variation in LE and TE concerning head, efficiency, and power in pump mode

### *3.2 Turbine Mode*

Figure 11 shows the numerical characteristic curve in turbine mode. The numerical results were compared based on the calculation performed in a previous study [27]. The head and power curve have an increasing trend, while the efficiency is concave downward, as in pump mode. Analyzing, if a higher mass flow rate is introduced, the pump could deliver more power, but the efficiency would decrease, so the energy conversion would not be appropriate. Therefore, it is preferable to operate the PAT at points close to the BEP. On the other hand, a flow rate lower than 18 $m^3/h$ and higher than 60 $m^3/h$ presents efficiencies from 5% to 80% lower. At the BEP, the power was calculated as 3.12 kW, a maximum efficiency of 50.49%, and a head of 51.65 m, which represents a relative error of 9.95% and an absolute error of 5.14 m.

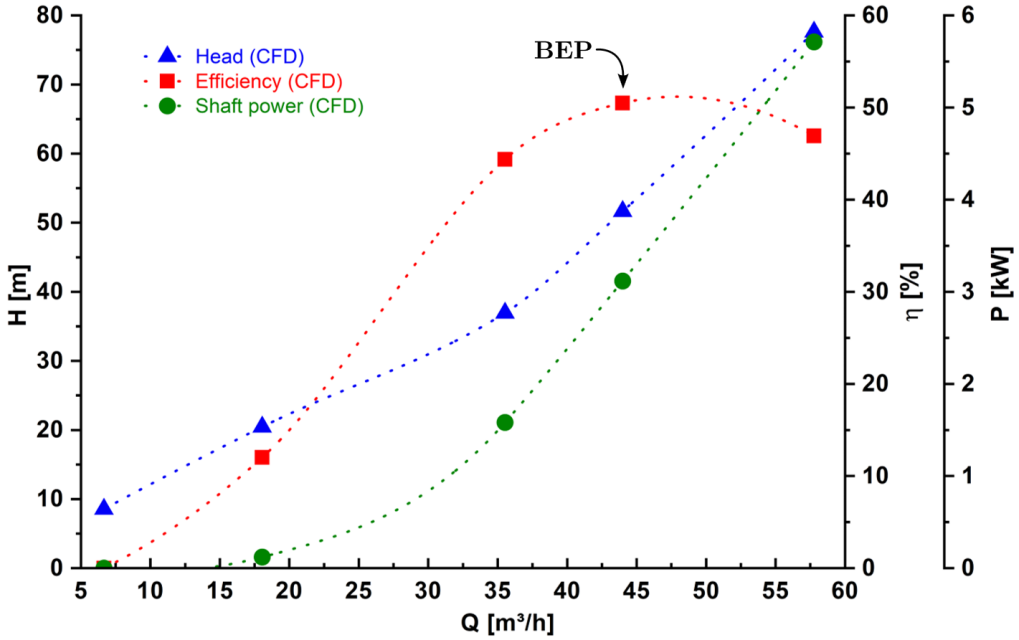


**Fig. 11.** Numerical curve in turbine mode [27]

Figure 12 shows the pressure and velocity contours in the cross-section view, meridional view, blade-to-blade view, LE, and TE. On the left, pressure contours of the PAT are observed. Pressure is in the range of 56 kPa to 546 kPa. In the suction until the impeller, the pressure decreases to a value from 546 kPa to 400 kPa and gradually decreases to 56 kPa while the fluid flows through the blades. In this mode, pressure is lower than pump mode. However, the meridional view and blade-to-blade view present maximum values close to 400 kPa, because the pressure of the fluid is transformed into kinetic energy by the impeller. The maximum pressure near the LE region was close to 400 kPa due to the interface between both components of the machine. The pressure located in TE was around 100 kPa due to the atmospheric pressure outlet condition. In comparison with Figure 9, the maximum pressure experienced by the PAT was 42% higher. However, the hydraulic head required at the BEP was 2.7 times higher. On the right, velocity contours are observed. Velocity is in the range of 0 m/s to 30 m/s. As the fluid enters the impeller, the velocity increases sharply to 30 m/s in LE. Next, velocity suddenly decreases due to the energy transformation into mechanical energy. The meridional view and blade-to-blade view present intermediate values close to 5 m/s. The TE region obtained a velocity between 5 and 7 m/s. In comparison, velocity on the blade surface was 28% lower to pump mode. It was due to the rotational velocity being 1382 rpm. However, velocity in turbine mode was 2.14 times higher than in pump mode.

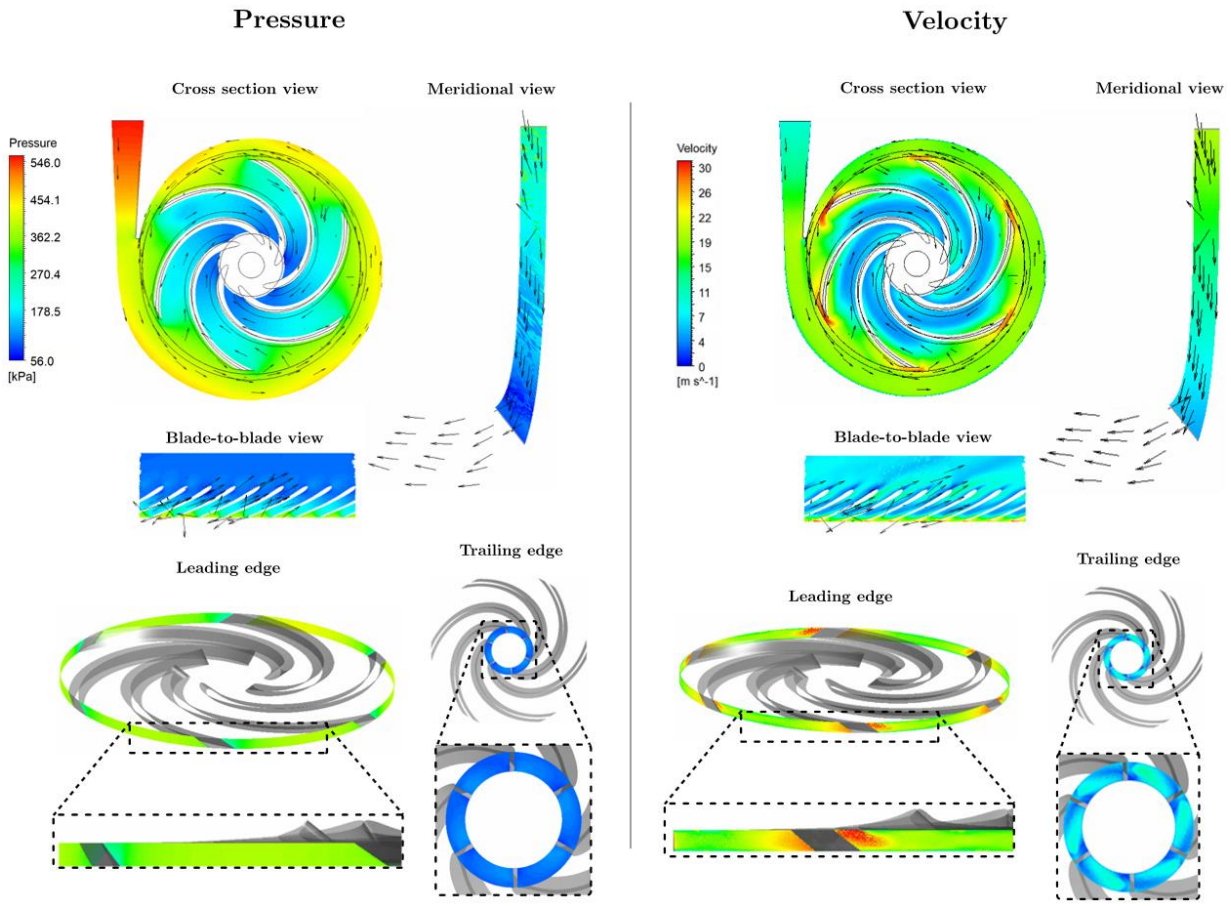


**Fig. 12.** Pressure and velocity contours in turbine mode

Figure 13 shows the behavior of inclination angle variation in LE and TE concerning head, efficiency, and power variables in turbine mode. Because shroud LE had a special variation, the comparison points of 25° coincide with the simulation conditions of 90° for LE. A decreasing trend could be observed concerning all three variables when the angle increased. This contrasts with the results in pump mode because the LE inclination causes the system to be more efficient, and more power can be obtained. However, it is possible to observe that an angle of less than 45° increases the hydraulic head of the turbine, which would require a higher site for installation in a practical case. In conclusion, the head increased to 6.83% and efficiency until 7.74% when the angle decreased, while the power was 13.38% greater. Therefore, reducing the angle in all cases makes the PAT suitable for generating electricity, but in pump mode would be unfeasible.

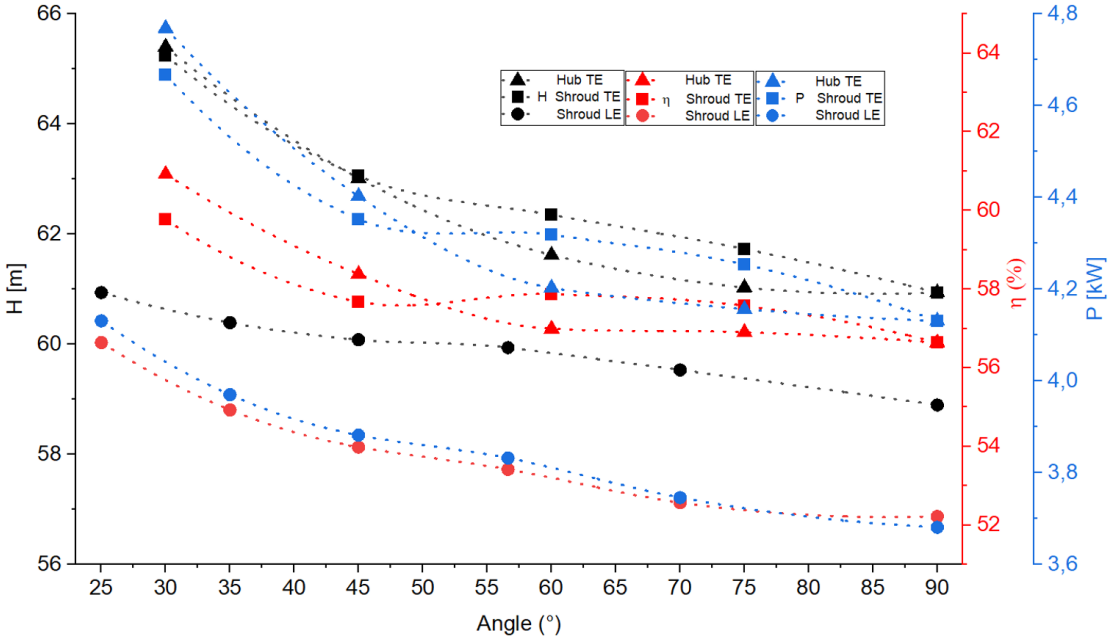


**Fig. 13.** Angle variation in LE and TE concerning head, efficiency, and power in turbine mode

## 4. Conclusions

In order to guarantee the fluid-dynamic results, the commercial pump simulations were compared with the experimental characteristic curve provided by manufacturer, getting a relative error of 6.29% in efficiency at the BEP, which is lower than the 10% proposed. Therefore, it provided us the possibility of analyzing the turbomachine in turbine mode and the modifications proposed to the blade leading and trailing edge angles, due to the numerical reliability reached.

Geometric modifications in pump mode produced a decrease in pumping capacity for cases where the angle was less than 90° at the trailing edge. The efficiency at 30° decreased to 17.6%. On the other hand, the variation of the leading edge was 2.8%, so the variation is negligible. Therefore, in pump mode, modifying the inclination of the trailing edge causes the turbomachine to lose hydraulic efficiency, and the leading edge does not have a relevant effect.

In turbine mode, when the angle decreases to 30°, the power increased 13.38%. On the other hand, the efficiency increases up to 7.74%. However, the hydraulic head required for a practical installation increased by 6.83%, which extends between 30° and 45°. Therefore, the impeller modification is valid for an angle greater than 45°.

It was evidenced that the geometrical modifications in the leading and trailing edges caused an inverse behavior in both operation modes. Reducing the angle in all cases makes the PAT suitable for generating electricity, but in pump mode would not be effective.

## Acknowledgment

The authors would like to thank the Advanced Materials and Energy research group (MATyER), especially the research line of Advanced Computing and Digital Design and Manufacturing Processes (SeCADD-ProM) and the system department of the Metropolitan Technological Institute (ITM), for allowing the use of the computer equipment and licenses of the Ansys® software to perform the simulations.

## References

[1] Fitriyana, Deni Fajar, Samsudin Anis, Abdul Rachman Al Qudus, Mirza Aufa Nugraha Lakuy, Rifky Ismail, Sri Nugroho, Gunawan Dwi Haryadi, Athanasius Priharyoto Bayuseno, and Januar Parlaungan Siregar. "The Effect of Post-Heat Treatment on The Mechanical Properties of FeCrBMnSi Coatings Prepared by Twin Wire Arc Spraying (TWAS) Method on Pump Impeller From 304 Stainless Steel." *Journal of Advanced Research in Fluid Mechanics and Thermal Sciences* 93, no. 2 (2022): 138-147. https://doi.org/10.37934/arfmts.93.2.138147

[2] Graciano-Uribe, Jonathan, Jorge Sierra, and Edwar Torres-López. "Instabilities and influence of geometric parameters on the efficiency of a pump operated as a turbine for micro hydro power generation: A review." *Journal of Sustainable Development of Energy, Water and Environment Systems* 9, no. 4 (2021): 1-23. https://doi.org/10.13044/j.sdewes.d8.0321

[3] Krenn, Jürgen, Helmut Keck, and Manfred Sallaberger. "Small and mid-size pump-turbines with variable speed." *Energy and Power Engineering* 5, no. 1 (2013): 48-54. https://doi.org/10.4236/epe.2013.52A007

[4] Vásquez, Diego Penagos, and Daniel Sanín Villa. "Parametric and Economic Analysis of a Pumped Storage System Powered by Renewable Energy Sources." *Journal of Advanced Research in Fluid Mechanics and Thermal Sciences* 84, no. 1 (2021): 43-59. https://doi.org/10.37934/arfmts.84.1.4359

[5] Barbarelli, S., M. Amelio, and G. Florio. "Experimental activity at test rig validating correlations to select pumps running as turbines in microhydro plants." *Energy Conversion and Management* 149 (2017): 781-797. https://doi.org/10.1016/j.enconman.2017.03.013

[6] Barbarelli, Silvio, Mario Amelio, and Gaetano Florio. "Using a statistical-numerical procedure for the selection of pumps running as turbines to be applied in water pipelines: Study cases." *Journal of Sustainable Development of Energy, Water and Environment Systems* 6, no. 2 (2018): 323-340. https://doi.org/10.13044/j.sdewes.d5.0181

[7] Derakhshan, Shahram, and Ahmad Nourbakhsh. "Experimental study of characteristic curves of centrifugal pumps working as turbines in different specific speeds." *Experimental Thermal and Fluid Science* 32, no. 3 (2008): 800-807. https://doi.org/10.1016/j.expthermflusci.2007.10.004

[8] Yang, Sun-Sheng, Shahram Derakhshan, and Fan-Yu Kong. "Theoretical, numerical and experimental prediction of pump as turbine performance." *Renewable Energy* 48 (2012): 507-513. https://doi.org/10.1016/j.renene.2012.06.002

[9] Huang, Si, Guangqi Qiu, Xianghui Su, Junrong Chen, and Wenlang Zou. "Performance prediction of a centrifugal pump as turbine using rotor-volute matching principle." *Renewable Energy* 108 (2017): 64-71. https://doi.org/10.1016/j.renene.2017.02.045

[10] Barbarelli, Silvio, Vincenzo Pisano, and Mario Amelio. "Development of a Predicting Model for Calculating the Geometry and the Characteristic Curves of Pumps Running as Turbines in Both Operating Modes." *Energies* 15, no. 7 (2022): 2669. https://doi.org/10.3390/en15072669

[11] Miao, Sen-chun, Jun-hu Yang, Guang-tai Shi, and Ting-ting Wang. "Blade profile optimization of pump as turbine." *Advances in Mechanical Engineering* 7, no. 9 (2015): 1687814015605748. https://doi.org/10.1177/1687814015605748

[12] Plua, Frank, Victor Hidalgo, P. Amparo López-Jiménez, and Modesto Pérez-Sánchez. "Analysis of Applicability of CFD Numerical Studies Applied to Problem When Pump Working as Turbine." *Water* 13, no. 15 (2021): 2134. https://doi.org/10.3390/w13152134

[13] Sánchez-Ríos, Carlos Andrés, Jonathan Graciano-Uribe, Sebastián Vélez García, and Diego Andrés Hincapié-Zuluaga. "Comparative analysis between a discrete spiral chamber and a continuous spiral chamber via ansys." *Tecciencia* 12, no. 23 (2017): 25-32. https://doi.org/10.18180/tecciencia.2017.23.4

[14] Burbano-Hernández, Andrés, Diego Hincapié, Jonathan Graciano-Uribe, and Edwar Torres-López. "Effect of the opening and location ratio on the performance of an H-Darrieus VAWT." *Revista Facultad de Ingeniería, Universidad de Antioquia* 104 (2022): 33-41. https://doi.org/10.17533/udea.redin.20210737

[15] Cifuentes, Oscar Darío Monsalve, Jonathan Graciano Uribe, and Diego Andrés Hincapié Zuluaga. "Numerical Simulation of a Propeller-Type Turbine for In-Pipe Installation." *Journal of Advanced Research in Fluid Mechanics and Thermal Sciences* 83, no. 1 (2021): 1-16. https://doi.org/10.37934/arfmts.83.1.116

[16] Fernández, J., R. Barrio, E. Blanco, J. L. Parrondo, and A. Marcos. "Numerical investigation of a centrifugal pump running in reverse mode." *Proceedings of the Institution of Mechanical Engineers, Part A: Journal of Power and Energy* 224, no. 3 (2010): 373-381. https://doi.org/10.1243/09576509JPE757

[17] Huang, Si, Guangqi Qiu, Xianghui Su, and Guowei Ou. "Flow performance analysis on shutoff condition in centrifugal pump based on CFD simulation." In *2014 ISFMFE-6th International Symposium on Fluid Machinery and Fluid Engineering*, pp. 1-5. IET, 2014. https://doi.org/10.1049/cp.2014.1142

[18] Neelambika, Neelambika, and Veerbhadrappa Veerbhadrappa. "CFD ANALYSIS OF MIXED FLOW IMPELLER." *International Journal of Research in Engineering and Technology* 3, no. 3 (2014): 601-607. https://doi.org/10.15623/ijret.2014.0315112
[19] Penagos-Vásquez, Diego, Jonathan Graciano-Uribe, and Edward Torres. "Characterization of a Commercial Axial Flow PAT Through a Structured Methodology Step-by-Step." *CFD Letters* 14, no. 1 (2022): 1-19. https://doi.org/10.37934/cfdl.14.1.119
[20] Qian, Zhongdong, Fan Wang, Zhiwei Guo, and Jie Lu. "Performance evaluation of an axial-flow pump with adjustable guide vanes in turbine mode." *Renewable Energy* 99 (2016): 1146-1152. https://doi.org/10.1016/j.renene.2016.08.020
[21] Derakhshan, Shahram, Bijan Mohammadi, and Ahmad Nourbakhsh. "Efficiency improvement of centrifugal reverse pumps." *Journal of Fluids Engineering* 131, no. 2 (2009). https://doi.org/10.1115/1.3059700
[22] Yang, Sun-Sheng, Fan-Yu Kong, Hao Chen, and Xiang-Hui Su. "Effects of blade wrap angle influencing a pump as turbine." *Journal of Fluids Engineering* 134, no. 6 (2012). https://doi.org/10.1115/1.4006677
[23] Li, Wei, Xiaofan Zhao, Weiqiang Li, Weidong Shi, Leilei Ji, and Ling Zhou. "Numerical prediction and Performance experiment in an engine cooling water pump with different blade outlet widths." *Mathematical Problems in Engineering* 2017 (2017). https://doi.org/10.1155/2017/8945712
[24] Peng, Guangjie, Qiang Chen, Ling Zhou, Bo Pan, and Yong Zhu. "Effect of blade outlet angle on the flow field and preventing overload in a centrifugal pump." *Micromachines* 11, no. 9 (2020): 811. https://doi.org/10.3390/mi11090811
[25] Sen-Chun, Miao, Shi Zhi-Xiao, Wang Xiao-Hui, Shi Feng-Xia, and Shi Guang-Tai. "Impeller meridional plane optimization of pump as turbine." *Science Progress* 103, no. 1 (2020): 0036850419876542. https://doi.org/10.1177/0036850419876542
[26] KSB. "Dry-Installed Pump MegaCPK." *KSB Inc*. December 1, 2022. https://www.ksb.com/en-us/lc/products/pump/dry-installed-pump/megacpk/M48A.
[27] Vásquez, Diego Penagos, Jonathan Graciano Uribe, Sebastián Vélez García, and Jorge Sierra del Rio. "Characteristic Curve Prediction of a Commercial Centrifugal Pump Operating as a Turbine Through Numerical Simulations." *Journal of Advanced Research in Fluid Mechanics and Thermal Sciences* 83, no. 1 (2021): 153-169. https://doi.org/10.37934/arfmts.83.1.153169
[28] Celik, Ishmail B., Urmila Ghia, Patrick J. Roache, and Christopher J. Freitas. "Procedure for estimation and reporting of uncertainty due to discretization in CFD applications." *Journal of Fluids Engineering-Transactions of the ASME* 130, no. 7 (2008). https://doi.org/10.1115/1.2960953
[29] Velásquez, Laura, Alejandro Posada, and Edwin Chica. "Surrogate modeling method for multi-objective optimization of the inlet channel and the basin of a gravitational water vortex hydraulic turbine." *Applied Energy* 330 (2023): 120357. https://doi.org/10.1016/j.apenergy.2022.120357
[30] Velásquez, Laura, Alejandro Posada, and Edwin Chica. "Optimization of the basin and inlet channel of a gravitational water vortex hydraulic turbine using the response surface methodology." *Renewable Energy* 187 (2022): 508-521. https://doi.org/10.1016/j.renene.2022.01.113
[31] Štefan, David, Mosè Rossi, Martin Hudec, Pavel Rudolf, Alessandra Nigro, and Massimiliano Renzi. "Study of the internal flow field in a pump-as-turbine (PaT): Numerical investigation, overall performance prediction model and velocity vector analysis." *Renewable Energy* 156 (2020): 158-172. https://doi.org/10.1016/j.renene.2020.03.185
[32] Ansys, C. F. X. "Solver modeling guide, Release 14.0." *Ansys Inc., Canonsburg* (2011).
[33] Yoon, Gil Ho. "Topology optimization method with finite elements based on the k-ε turbulence model." *Computer Methods in Applied Mechanics and Engineering* 361 (2020): 112784. https://doi.org/10.1016/j.cma.2019.112784
[34] Ghorani, Mohammad Mahdi, Mohammad Hadi Sotoude Haghighi, Ali Maleki, and Alireza Riasi. "A numerical study on mechanisms of energy dissipation in a pump as turbine (PAT) using entropy generation theory." *Renewable Energy* 162 (2020): 1036-1053. https://doi.org/10.1016/j.renene.2020.08.102
[35] Yusuf, Siti Nurul Akmal, Yutaka Asako, Nor Azwadi Che Sidik, Saiful Bahri Mohamed, and Wan Mohd Arif Aziz Japar. "A short review on rans turbulence models." *CFD Letters* 12, no. 11 (2020): 83-96. https://doi.org/10.37934/cfdl.12.11.8396
[36] Huang, P., J. Bardina, and T. Coakley. "Turbulence modeling validation, testing, and development." *NASA Technical Memorandum* 110446 (1997): 10-2514. https://doi.org/10.2514/6.1997-2121
[37] Ismail, Mohd Azlan, Al Khalid Othman, and Hushairi Zen. "Numerical simulation on end suction centrifugal pump running in inverse flow for microhydro applications." In *Applied Mechanics and Materials*, vol. 773, pp. 358-362. Trans Tech Publications Ltd, 2015. https://doi.org/10.4028/www.scientific.net/AMM.773-774.358
[38] Qian, Zhongdong, Fan Wang, Zhiwei Guo, and Jie Lu. "Performance evaluation of an axial-flow pump with adjustable guide vanes in turbine mode." *Renewable Energy* 99 (2016): 1146-1152. https://doi.org/10.1016/j.renene.2016.08.020

[39] Mott, Robert L. *Mecánica de fluidos aplicada*. Pearson Educación, 2006.
[40] ANSYS. "2.3.1 The Multiple Reference Frame Model." *ANSYS Inc*. Accessed April 22, 2023. https://www.afs.enea.it/project/neptunius/docs/fluent/html/th/node33.htm.
[41] Lorusso, Michele, Tommaso Capurso, M. Torresi, B. Fortunato, F. Fornarelli, S. M. Camporeale, and Rosario Monteriso. "Efficient CFD evaluation of the NPSH for centrifugal pumps." *Energy Procedia* 126 (2017): 778-785. https://doi.org/10.1016/j.egypro.2017.08.262
[42] Ghorani, Mohammad Mahdi, Mohammad Hadi Sotoude Haghighi, Ali Maleki, and Alireza Riasi. "A numerical study on mechanisms of energy dissipation in a pump as turbine (PAT) using entropy generation theory." *Renewable Energy* 162 (2020): 1036-1053. https://doi.org/10.1016/j.renene.2020.08.102
[43] Claudio, Mataix. "Turbomáquinas hidráulicas." *Ed. ICAI, Madrid-Spain* (1975).
[44] Mataix, Claudio. *Fluid mechanics and hydraulic machines*. Harla, 1982.